Arabian Journal for Science and Engineering (2023) 48:12523–12539
https://doi.org/10.1007/s13369-023-07735-7

RESEARCH ARTICLE-MECHANICAL ENGINEERING

Tri-Rotor Propeller Design Concept, Optimization and Analysis of the Lift Efficiency During Hovering

L. Piancastelli[1] · **M. Sali**[1]

Received: 18 August 2022 / Accepted: 15 February 2023 / Published online: 8 May 2023

Abstract

This study introduces the simulation of a tri-rotor contra-rotating propeller for thrust force and hover lift efficiency during vertical take-off. Vertical take-off or landing is a method used by many aircraft and makes the vehicle more convenient and easier to use. The second rotor revolved in the opposite direction of the first and third rotors. The proposed multi-rotor system has NACA 0012 untwisted and symmetric airfoil and includes three rotors with two blades for each. The airflow analysis was optimized with computational fluid dynamics simulation by using different pitch combinations to achieve the highest hover lift efficiency with sufficient overall thrust value. The critical angle of attack for the chosen airfoil gave the boundary conditions for the pitch of rotors. The results showed us that the most efficient combinations for three rotors work better with an increase of pitch angle from top to bottom so that there is a difference of at least two degrees between propellers. Experiments with angles of attack within the boundary conditions showed that the blade combinations starting from three degrees and increasing values gave positive and adequate results in many cases. In addition, the results showed that a regular increase in the angle of attack does not relate to a regular increment in thrust force.

Keywords Multi-rotor propeller · Coaxial propeller · Tiltrotor · Airfoil · Thrust force · Hovering · Hover lift efficiency · Optimization · Disc loading

List of Symbols

G (kg)	Gross weight
G (m/s^2)	Gravity
k	Safety factor
S	Number of propellers
Δ (m^2)	Thrust area of the propeller
ϵ	Tri-rotor
V (m/s)	Rotor speed
Ω (rad/s)	Rotor angular speed
F (N)	Thrust force

1 Introduction

The vast majority of unmanned aerial vehicles (UAVs) have a multi-rotor configuration to complete the hovering and vertical take-off or landing [1]. There are several examples of coaxial-rotor designs, such as curved rotors and other VSTOL (vertical/short take-off–landing) that have proven suitable for helicopters [2]. A coaxial propeller design has some cases (Fig. 1) with fixed wing aircraft such as the Supermarine Spitfire (mk.XIX), Tupolev Tu-95 bomber (known as the bear), the Fairey Gannet and the Avro Shackleton [3]. Rotor efficiency of VTOL vehicles is high compared with other lifting aircrafts due to the massive mass flow through the rotors during hovering. Even in the low speed the coaxial helicopter rotors have better performance than single rotors. Considering this advantage, Kamov coaxial-rotor helicopters were developed, as shown in Fig. 1b [4].

Regarding modern helicopter systems, conventional and multi-rotor configurations have advantages of they own. For conventional helicopters, a single main rotor or single tail

✉ L. Piancastelli
luca.piancastelli@unibo.it

M. Sali
merve.sali2@unibo.it

[1] DIN, Università degli Studi di Bologna, Viale Risorgimento 2, Bologna, Italy

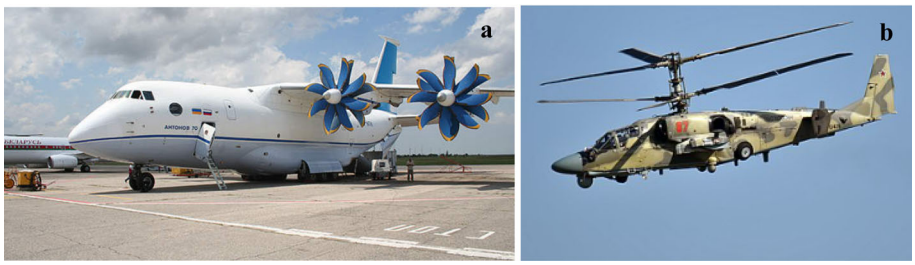

Fig. 1 Coaxial dual-rotor configurations. **a** Antonov-70 with contra-rotating propellers, **b** Kamov-52 with coaxial rotors

rotor can be given as an example while multi-rotor configurations express tandem or tilt-rotor aircraft. Both systems are widely used in military and civil applications [5].

However, considerable performance is achievable with a well-designed propeller which is the essential factor of the system [2]. Similarly, the cruise efficiency can rise with the proper propeller design parameters by increasing the propeller efficiency during the cruise flight [6]. Likewise, coaxial design alleviates the detrimental effects of the retreating blade of conventional helicopters, high-speed performance and critical cruise efficiency [7–11]. A coaxial-rotor helicopter layout shows substantial advantages compared with the conventional single-rotor configuration. It is known that double-rotor, contra-rotating propeller applications are increasing in the military field. In helicopters, the torque of a coaxial-rotor system can be balanced by the two contra-rotating rotors, taking over the need for a tail rotor. Thus, the additional weight and power consumption associated with the tail rotor can be saved [8].

Additionally, a coaxial-rotor design has the potential to lighten the adverse effects of retreating blade stalls. The rotor disc has two main areas, namely the advancing side and the retreating side. And the relative airflow during the forward speed of the helicopter is higher over the advancing side, but lower at the retreating side. Moreover, this situation occurs with a higher angle of attack at high-speed flights and restricts the propulsive flight speed of a helicopter. In this regard, a second contra-rotating propeller helps to offset the lift towards both sides of the rotor disc [11, 12].

Moreover, the coaxial rotor has three essential advantages in a helicopter. The first one is that it removes the requirements for an anti-torque system, the second one is the rotor diameter can be scaled down when compared with a single rotor and the third one is not having the instability region that causes the "settling with power" condition [13]. Experimental analysis showed that instabilities in the single-rotor design [14] can be eliminated by the addition of a second rotor. The second propeller reduces the instability of the first propeller, by reducing the instability in the vortex ring state [15]. These three advantages give the possibility of more efficiency at most flying conditions while providing a smaller size of the aircraft. In addition, the coaxial layout offers more advantages [2, 16, 17]. It can provide higher forward speeds than a conventional helicopter. In a tilt-rotor layout, a coaxial-rotor propeller may present some benefits [18], such as better aerodynamic and weight efficiency [7, 19, 20]. The research of Coleman [21] studied a summary of aerodynamic performance and wake characteristics of the coaxial rotor regarding experimental and theoretical findings; Ramasamy [22] found a 5% reduction in a stacked rotor power by using 7% diameter axial space while the thrust is the same with a coplanar rotor; Serrano et. al. [1] explained the multi-rotor vehicle condition in the case of forwarding flight. It creates a propeller thrust parameter by tilting the rotor disc in the direction of motion. Ferguson [23] made a research on multiple helicopter configurations in terms of performance, dynamic stability, manoeuvrability and handling qualities and investigated the development of compound helicopter configurations. This proved that compounding configuration for thrust increases the forward propulsion thanks to the axial thrust the propellers provide. In addition, the addition of wings to the design has adverse effects on the hover performance of the component helicopter. Another critical performance-related consequence is that it displays unstable longitudinal movements at high-speed flights. Furthermore, a compound helicopter has more promising results in terms of manoeuvrability than a conventional one.

Likewise, the coaxial propeller system has some advantages over the smaller-sized aircraft design when compared to two single rotors mounted side by side. Thus, the efficiency of the contra-rotating propeller system during a forwarding flight needs more detailed research for better recognition [24]. Moreover, the advantages and high performance of the coaxial propeller are the main reasons to study multi-rotor propellers in this research. The benefits of this system over the other designs claimed to research another version of this design; the *tri-rotor system*. One of the most notable advantages of this design is a third propeller that reduces the diameter of the propellers while increasing the system ergonomics. Furthermore, it is aimed to design a tri-rotor propeller as an alternative to the coaxial propeller and it has been ensured that this unimplemented design leads to innovations based on the results it has.

Therefore, in this study, the aim was to simulate three coaxial rotors using CFD (computational fluid dynamics) method. A solution whether the same or greater efficiency

Table 1 Design assumptions of propeller system

	Tri-rotor propeller
Aircraft type	Tilt–Rotor
Hover lift efficiency	3–4
Rotor distance	350 mm
Airfoil type	NACA 0012
Propeller rotation	Coaxial
Initial angle of attack	3.3 DEG

can be achieved with the smaller rotor area provided by the tri-rotor propeller beyond the coaxial propeller is going to be portrayed. One of the main goals of this design is to divide the power between the three rotors so that technical malfunction during flight may lower the effect in flight performance. With flow simulation, it is possible to calculate the thrust force with several different angle values. A wide variety of blade angle combinations were evaluated to understand the aerodynamic performance of the tri-rotors. The optimization process aims (1) to optimize our contra-rotating propeller design; (2) to perform the airflow analysis of the entire design for the different pitch angles, calculate the thrust and torque values for each propeller; and finally (3) to choose the most efficient configuration of the system by calculating hover lift efficiency during hovering.

2 Materials and Methods

2.1 Geometry Description of the Propeller Design

The first step in the propeller design is to define the aircraft type and desired working condition. All assumptions and determined values are given in Table 1. All the details about the chosen values are explained in this section.

The graph shown in Fig. 2 can be used to determine the aircraft type. As seen from this graph, DL (disc loading) and HLE (hover lift efficiency) values are the major values to be identified. Disc loading represents the average pressure change through rotor disc. Hover efficiency is the relation between the weight of an aerial vehicle and the power required to keep it suspended in the air. Our design targets tilt-rotor performance.

As defined before, tilt-rotor values are the target, and in this case, as seen from the graph, the HLE value must be around 3–4. Similarly, DL can be chosen from Fig. 1. On the other hand, the UH1 helicopter is the reference system for our innovative design, because this helicopter is already in use of the military and has valid tilt-rotor efficiency. Its design condition and parameters have been used to create a new propeller system. The required values, such as Mach

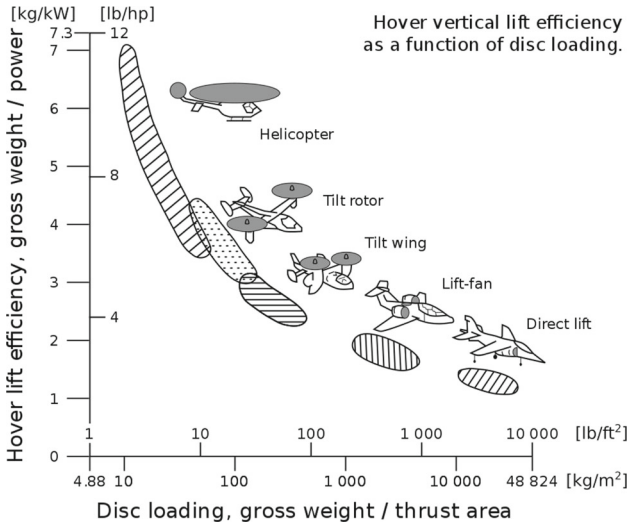

Fig. 2 Magnetization as a function of applied fields [25]

Table 2 Initial values of propeller system

	UH1C propeller	Tri-rotor propeller
Lift	35,804 N	
Total weight	3651 kg	250 kg [27]
Torque	1000 HP	
Radius of propeller	14.63 m	
Rotor speed	33.929 rad/s	188.32 rad/s
Tip speed	248 m/s	248 m/s
Number of rotor	1	3
Number of blades	2	2
Tip Mach number	0.8	0.8
Humidity	0%	0%
Disc loading (DL)	224 kg/m^2	224 kg/m^2

number, tip speed and number of blades, were derived from UH1 [26]. The values used in this design are given in Table 2. In the following steps, how these values are found will be explained.

Taking into consideration to an innovative design, the diameter of the tri-rotor system was calculated using the same disc loading value of the UH1. The disc loading value for a hovering helicopter is determined by dividing the helicopter weight (G) by the area swept by the blades of a rotor (Δ).

For this, the gross weight of UH1 and the thrust area of the current blades were used. As known, the weight of a UH 1 helicopter is 3651 kg, and power can reach a maximum of 1000 HP due to the torque limiter [26].

$$\mathrm{DL\ (UH1)} = (G)/\Delta = 224\ \mathrm{kg/m^2}. \quad (1)$$

Table 3 Values determined by calculations

	Tri-rotor propeller
Diameter of rotor (D)	2.628 m
Lift (F)	3641.76 N

Then, the same disc loading value was used to calculate the propeller diameter. Design assembly for the tri-propeller design is referenced from [27].

$$\mathrm{DL(UH1)} = (G(\epsilon) \times g \times k)/(\Delta(\epsilon) \times S) \tag{2}$$

$$D\ (\text{Tri - rotor}) = 2.628\ \text{m}$$

where "k" is the safety factor here and "g" is gravity. From the calculations above, we found out that our radius is 1.315 m, and we can calculate our angular velocity as 188.32 rad/s. Then, the thrust force (F) needs to be obtained from the propeller calculation, and design geometry is also referenced from [27]. Thrust force is equal in this study to the gross weight of the helicopter (vertical force) divided by the number of rotors. In the case of the lift, thrust force is higher than the gross weight, and the helicopter would take off.

$$F(\epsilon) = (W \times g \times k)/(\cos 45^\circ \times S) = 3641.76\ \text{N}. \tag{3}$$

The missing data in Table 1 were completed, and the final values were obtained resulting in the values given in Table 3.

Afterwards, it is time to choose the proper airfoil which affects thrust force substantially. We preferred to use NACA 0012 airfoil (Fig. 3) with untwisted geometry, as it was used in other studies [28, 29].

2.2 Implementation of the Propeller Design

Two blades were used in each rotor as UH1. One of the most critical factors of the three-rotor propeller is the rotor distance. There are several studies where different ratios are applied [31–33]. According to these references and after a few simulations, we decided to use a distance equal to 13.3% of the rotor. The multi-rotor system was designed by using three multi-blade rotors. The first rotor blade was designed to rotate clockwise direction. Therefore, the second rotor rotates in an anticlockwise direction, and the bottom rotor rotates at the same direction as the top rotor (Fig. 4).

2.3 Simulation Environment

A simulation environment and simulation settings must be validated to simulate the tri-propeller design. To prove the validity of the CFD (computational flight dynamics) simulation, the rotor of the UH1C "HUEY" helicopter was simulated (Fig. 5). Therefore, SolidWorks Flow Simulation was preferred as a software to find out the lift performance and torque values. The data were taken from Tables 1, 2, 3 and 4. As a reference value, simulation results were evaluated according to the graph that shows the hover lift efficiency and disc loading in Fig. 2.

We created a pilot simulation environment to validate the simulation. One of the most important factors in these kinds of simulations is the environmental conditions. Therefore,

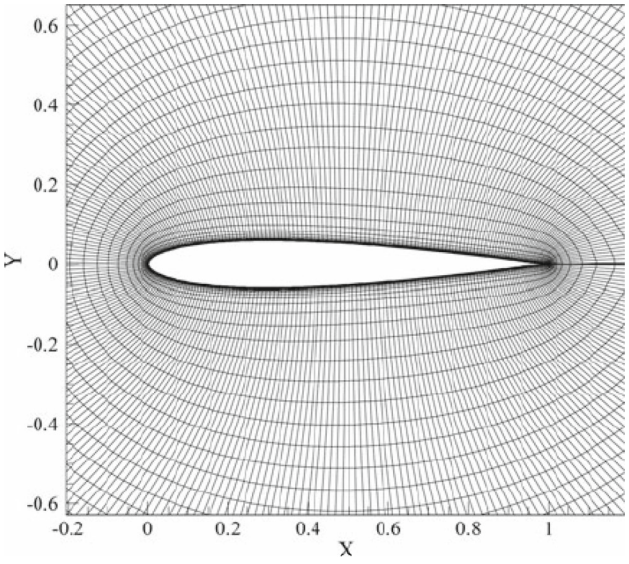

Fig. 3 The airfoil chosen for the tri-rotor propeller system: NACA 0012 airfoil [30]

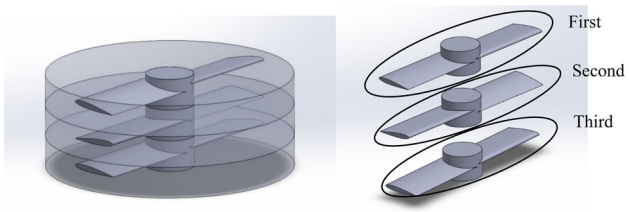

Fig. 4 Coaxial tri-rotor propeller design

Table 4 Environmental conditions for the simulation test

Altitude	0
Temperature offset	− 50 °C
Temperature	238.15 K
Pressure	1,401,325 Pa
Density	1.48219 kg/m^3
Speed of sound	309.364 m/s
Dynamic viscosity	0.0000155158 Pa/s

Fig. 5 UH1C "HUEY" helicopter (U.S. Army photograph from the official U.S. Department of the Army publication Vietnam Studies—Air mobility 1961–1971. Washington D.C. 1989)

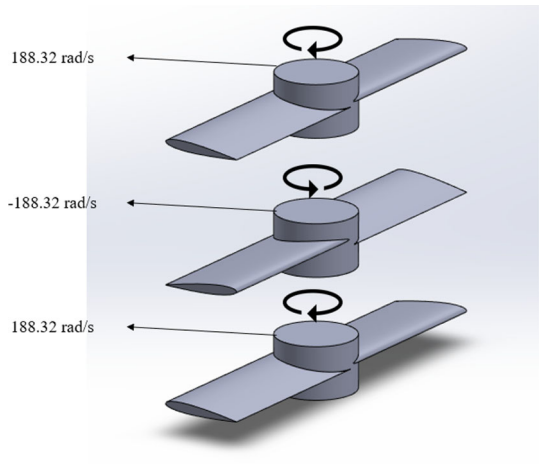

Fig. 7 CFD simulation rotational settings details

this study used the same values for UH1 (taken from ISA atmosphere calculator) [34] given in Table 4.

Figure 6 and Table 5 show the results with our simulation settings. As seen from the result, lighter green areas show lower pressure and yellow areas means higher pressure underside which proves the lift. And according to numerical results (Table 5), the desired lifting force is easily obtained by adjusting the attack angle.

2.4 Aerodynamic Simulation of Tri-Rotor Propeller System

We have implemented the same simulation settings on the tri-rotor propeller design. The proposed tri-rotor propeller design has three rotors which mean each rotor can have its angle of attack.

2.4.1 First Simulation

One of the most important parameters for each rotor is the angle of attack. To choose the collective pitch for the initial value, we used results from the research of Kusyumov et al. [35] as a reference. In the first simulation, an angle of attack of 3.3 DEG was chosen for the first propeller. For the second and third propellers, we chose 5.3 DEG and 3.3 DEG, respectively. The combinations of the blade settings are working better at + 2°/−2° [15]. In addition, the rotational speed and direction of the rotors are represented in Fig. 7. According to these settings, force and torque results are given in Table 6 Angle configuration display of blades is shown in Fig. 8.

The thrust value of the first simulation with the tri-rotor layout is 2924 N, and the power of the triple rotor is 258 HP.

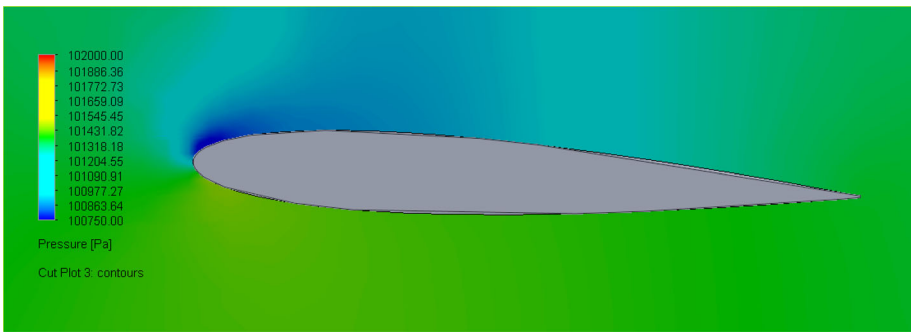

Fig. 6 Pressure distribution results of the Huey rotor blade

Table 5 Huey rotor simulation results

Diameter propeller (m)	Collective pitch (DEG)	Speed (rad/s)	Global force (N)	Power (HP)	Hover lift efficiency
14.63	2.8	33.9292	30,270	802	3.847
14.63	3.3	33.9292	36,656	863	4.33
14.63	4.0	33.9292	62,284	1172	5.4

Table 6 The results of the initial simulation

Diameter propeller (m)	Collective pitch (DEG)	Speed (rad/s)	Global force (N)	Power (HP)	Hover lift efficiency
2.628	3.3–5.3–3.3	188.32	2924	258	1.15

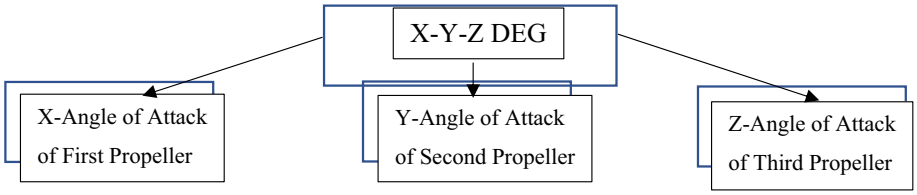

Fig. 8 Display of blade angles and combinations

Table 7 Final values of three propeller systems for the simulation

	UH1C propeller	Tri-rotor propeller
Lift	35,804 N	3641.78
Radius of propeller	14.63 m	2.628 m
Rotor speed	33.929 rad/s	154.682 rad/s
Tip speed	248 m/s	248 m/s
Number of rotor	1	3
Number of blades	2	2
Tip Mach number	0.8	0.657
Outside temperature	238.15 K	238.15 K
Humidity	0%	0%

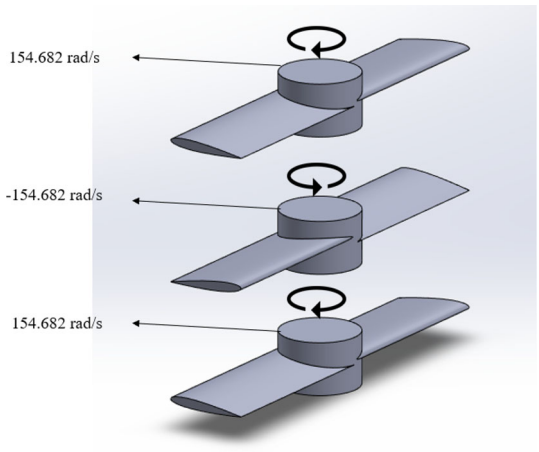

Fig. 9 CFD simulation rotational settings details with new values

According to these values, efficiency is lower than desired range. To increase the system lift efficiency, angular speed was decreased to create less power for each rotor. This situation was possible by the reduction of the Mach number. As a result, it had to be optimized to obtain the best values.

2.4.2 Second Simulation

According to the first simulation results, the power (HP) of the rotors has to be decreased. For these reasons, we optimized the angular velocity value. This optimization can be achieved by changing the Mach number (M). In the new case, we defined the Mach number as 0.657, and according to this given value, the new angular velocity was 154.682 rad/s. These new values were compared with the UH1C helicopter in Table 7.

With these new values and same environmental conditions, we performed our simulation once again (Fig. 9).

Figure 10 shows the airflow around the blades along the y-axis. Distribution of airflow area has decreased due to the reduced angular velocity but shows more vortices formed towards the tip of the propeller. Also, the air velocity decreased.

In this simulation case, the second and third propellers showed positive thrust values because of more pressure under the airfoil (Fig. 11). Numerical results (Table 8) showed global force and the total power of the tri-rotor together. The efficiency could not reach the desired value in the initial simulation.

As regards these results, the thrust value and power of the system decreased. On the other hand, HLE slightly increased. In conclusion, the hover lift efficiency still was not sufficient to reach the tilt-rotor standards. We performed several combinations to optimize the results to reach the targeted values. For this reason, an optimization method is performed to find the best design for the entire system.

2.5 Optimization of the Three Propeller Layout

The main objective is to find the tri-rotor design which provides optimum hover lift efficiency. To achieve that, the pitch of the rotors is the main parameter. For the tri-rotor, we needed to perform each combination of the blade angles according to the critical angle of attack of the chosen airfoil to find the best efficiency. Critical angle of attack is 8 DEG for NACA 0012 (Fig. 12) [36]. Thus, the blade pitch angle changed between 0° and 8°, and power and thrust coefficient calculations were done with different combinations.

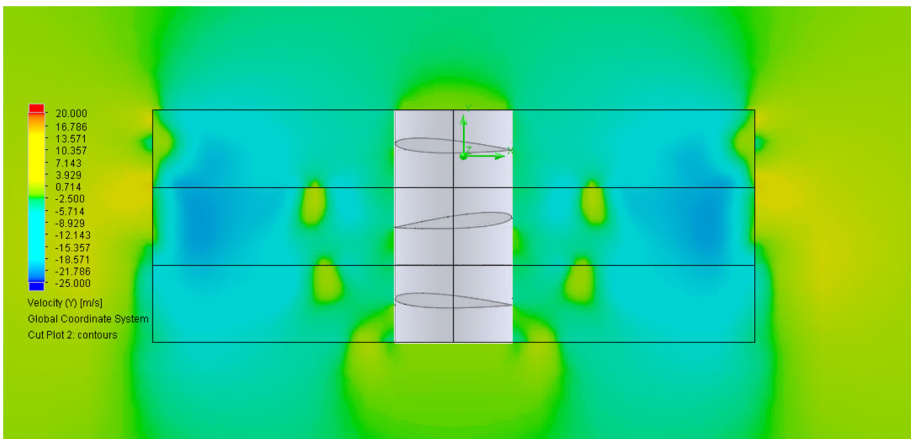

Fig. 10 Flow velocity result in the *y*-axis

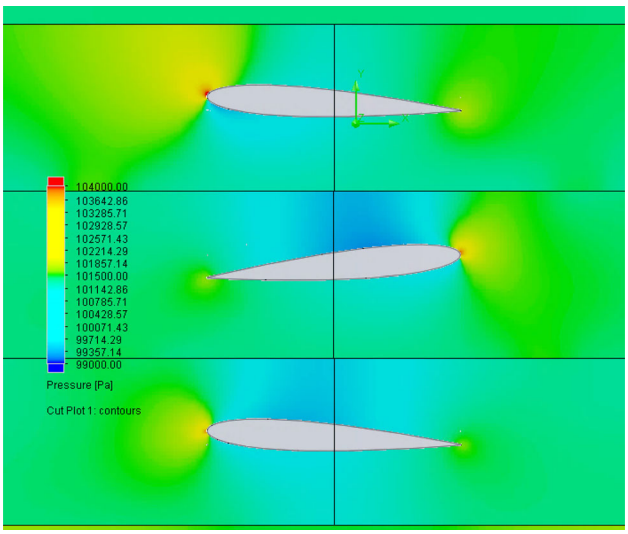

Fig. 11 Pressure distribution results of propeller design

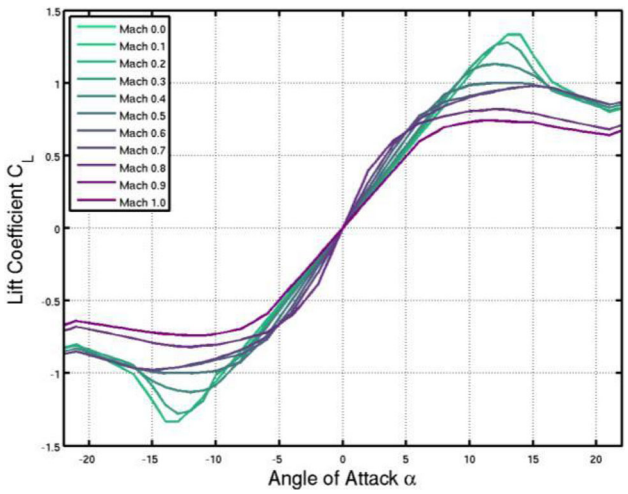

Fig. 12 The angle-of-attack graph of NACA 0012 Airfoil [36]

The angle-of-attack combination for the rotor blades was performed with a step of 1 DEG.

An exhaustive search method was used for the propeller design optimization. Exhaustive search, also called brute-force research, is a common problem-solving method aimed at generating and testing the problem [37, 38]. It includes an algorithmic approach that calculates all combinations systematically and analyses the results. All the possibilities were overseeing according to this method until reaching the best outcome. All simulations were performed by using the same boundary conditions. Identification of combinations was achieved by giving each rotor an angle from 0 to 8.

3 Results

Calculation outcome demonstrated that the propulsion efficiency of the propeller increases with the rotor angle-of-attack (AOA) increment [1]. Simultaneously, in this study, the results showed that the highest thrust was obtained by increasing the attack angles of the propellers from the first propeller to the third, or when the third propeller had a higher attack angle than the first and second propellers. Similarly, it is proven that each added rotor increases the overall thrust, even though it produces less force than the previous rotor [39]. However, there is a wide variety of angle-of-attack combinations with triple rotors, and the results are not as constant

Table 8 The results of optimized simulation

Diameter propeller (m)	Collective pitch (DEG)	Speed (rad/s)	Global force (N)	Power (HP)	Hover lift efficiency
2.628	3.3–5.3–3.3	154.682	1837.83	124	1.511

Table 9 Comparison of results of designs under different diameters and Mach numbers

Diameter propeller (m)	Collective pitch (DEG)	Mach number (M)	Speed (rad/s)	Global force (N)	Power (HP)	Hover lift efficiency
2.628	3.3–5.3–3.3	0.8	188.32	2924	258	1.15
2.628	3.3–5.3–3.3	0.657	154.682	1837.83	124	1.511
4.552	3.3	0.657	92.12	2888.561	149	1.976

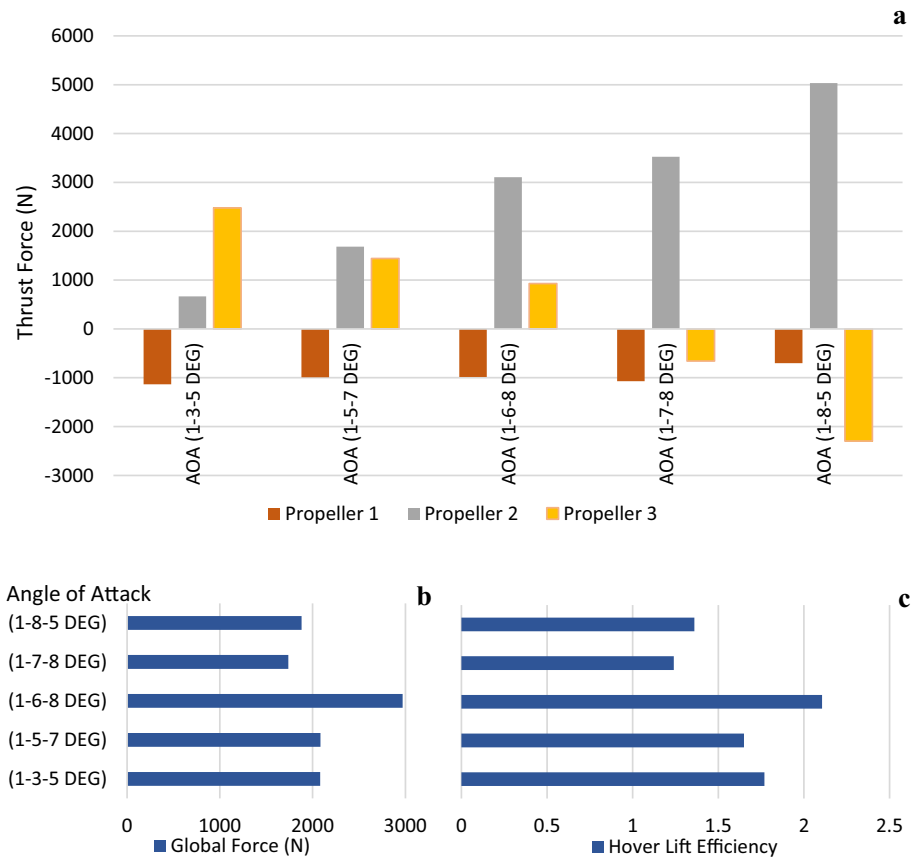

Fig. 13 **a** Thrust force graph, **b** global force graph, **c** hover lift efficiency graph when using 1 DEG on the first propeller

as in a single-rotor design; concluding that a coaxial arrangement produces less thrust when compared with a single rotor at the same propulsion power [40]. In addition, we know that the two systems have the same Mach number (0.657) (the first one is the single rotor with 4.5 m diameter of the disc and the other one is a tri-rotor with 2.6 m diameter); the smaller disc area produces less thrust (Table 9). In previous studies, it was stated that the loss of efficiency with decreasing the propeller diameter has been searched, and it was found out that the diameter of the propeller affects the efficiency of the rotor system. Thus, we found out that the same or closer efficiency values can be reached with smaller diameter values thanks to an increase of the number of rotors. Finally, when these two systems are compared, the efficiency of the first one is 1.976 and the tri-rotor efficiency is 1.511. Efficiency is more dependent on diameter, rather than angular speed [40].

3.1 Thrust Force and Hover Lift Efficiency

According to the results obtained from the simulations under all the combinations stated before, some essential inferences are:

1. In the case of 1 DEG for the first propeller, when we used a higher angle at the second and third propeller subsequently, the first propeller always showed a negative thrust (Fig. 13). This intrigued us to try with higher angles for the first propeller. An example of the pressure distribution created by using 1 DEG in the first propeller is shown in Fig. 14.

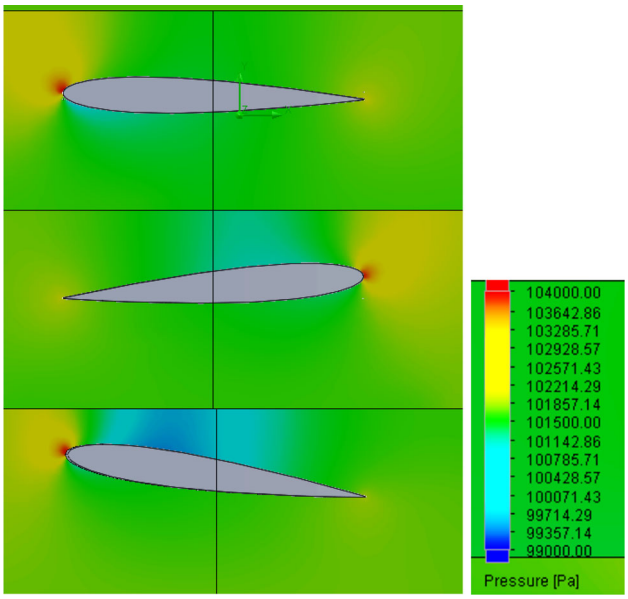

Fig. 14 Pressure distribution results of 1-4-8 DEG combination

Moreover, the thrust force graph (Fig. 13a) proves the negative results of the first propeller. Likewise, the global force values (Fig. 13b) and hover lift efficiency (Fig. 13c) are not sufficient for these configurations.

However, the pressure distribution results further establish that the first propeller has lower pressure on the underside than the upside, contrary to the second and third propellers; this situation means the first propeller works to create downforce while others create lift. This situation is shown in all 1 DEG combinations.

2. As the angle of attack of the third propeller decreased, the hover lift efficiency started to reduce. The results of the third propeller with 1 DEG combinations are shown to understand this extreme loss of thrust force. The third propeller always gives a negative value when 1 DEG combination is used (Fig. 15a). Also, efficiency is insufficient and below 1.5 (Fig. 15c).

In this case, there is a higher pressure found on the upper side of the airfoil of the third propeller. This caused a negative thrust overall (Fig. 16a, b). Also, the first and second propellers do not have regular results. In some cases, the first propeller may have a negative result overall (Fig. 16a).

Apart from these combinations, the results in the case of sliding the degree of the third propeller are given in Fig. 17a, b. Again, the third propeller was found to not provide high values at low degrees. Moreover, the hover lift efficiency decreased as the third propeller angle value was reduced from 8 to 1. It is worth noticing that the second propeller was

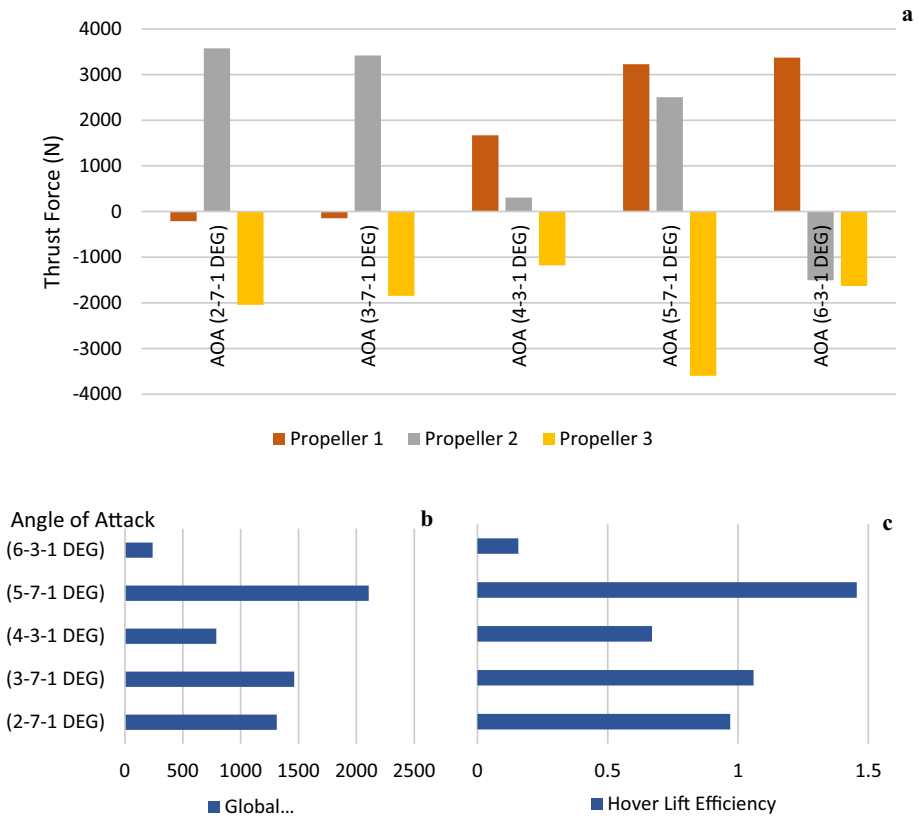

Fig. 15 **a** Thrust force graph, **b** global force graph, **c** hover lift efficiency graph when using 1 DEG on the third propeller

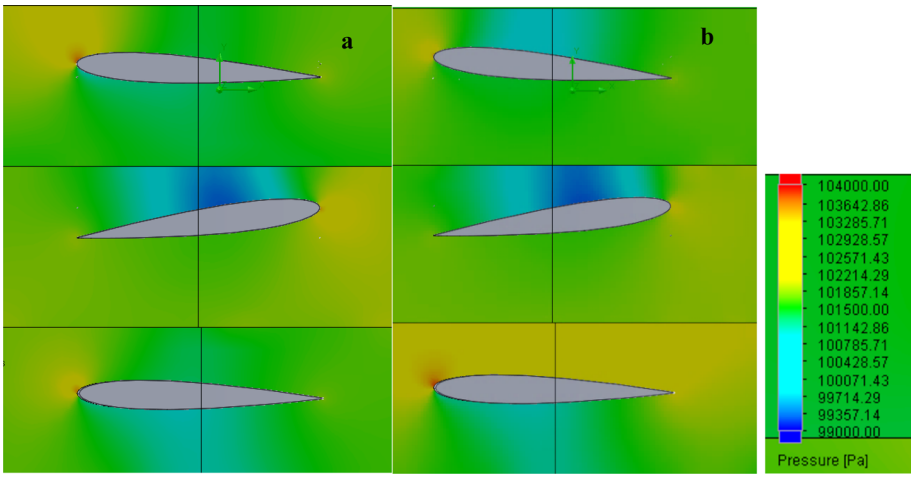

Fig. 16 Pressure distribution results of; **a** 3–7–1 DEG combination, **b** 5–7–1 DEG combination

always at the same angle, 7 DEG in Fig. 17a and 8 DEG in Fig. 17b. This specific part of the combination is shown in the latter graphs for a better understanding of the behaviour of the propellers.

3. When the AOA (angle of attack) increased in the first, second and third rotor, respectively, the system gave sufficient thrust for the lift values, especially at high angles in the second and third propeller. Moreover, the HLE is closer to the desired limits (between 3 and 4). But, in many combinations all propellers are not working in harmony since at least one of them showed a negative thrust (Fig. 18). However, the pressure results of 3–7–7 DEG combination have the best lift performance for the second propeller and a higher pressure as shown in Fig. 19. These results showed a conflict between the second and third propellers when having an equal angle-of-attack value.
4. Finally, for the best result scenario, in the case of increased rotor angles, we found sufficient thrust at certain angles, and the best results were outlined. The average value of hover lift efficiency is close to 3 for the successful combinations. In these combinations, each propeller gave positive results (Fig. 20) which represents the lift. The propeller on such combinations created a balanced force, while in others, a single propeller produced a higher lift. In the cases where a single propeller produces high thrust, the other propellers do not show strong results. In instances where two propellers create sufficient thrust, the thrust force of the third propeller is negligible. Additionally, HLE values are average between 2.5 and 3. Finally, from the flow velocity behaviours of the best propeller designs, the first and third propellers produced a higher lift force (Fig. 21). The second propeller, being the only propeller that rotates in the opposite direction, must both provide balancing and assist the thrust force. Therefore, its performance is more unstable in some cases.

Additionally, the blue areas in Fig. 21 are mostly more specific on the upside of the propellers. The highest pressure appears at the leading edge of the propellers. Moreover, there is a high rate of vortices at the trailing edge.

3.2 Thrust and Power Coefficient

The lift and power coefficient values were calculated to verify the numerical results of our design and to compare it with other studies. These values are independent of the number of blades or rotors used, as well as the type of airfoil used. The formula as defined in Eq. x is used,

$$C_{\mathrm{T}} = \frac{T}{\rho . A . V_{\mathrm{tip}}^2}$$

$$C_{\mathrm{P}} = \frac{P}{\rho . A . V_{\mathrm{tip}}^3}$$

where T is the thrust force, P is the power, ρ is the air density, A is the disc area and V_{tip} is the tip speed of the propeller.

This analysis was performed for combinations showing increased angles of attack; even if the ascending of coefficient values are not regular, they will show an irregular increment against an increment in attack angles (Fig. 22).

Ramasamy [5] compared the hover performance of single, coaxial, tandem and tilt-rotor configurations. Likewise, the NACA 0012 airfoil was used as the untwisted airfoil, similar to our study, but an additional highly twisted (xv-15) airfoil was used for each design. When we consider it as a similarity of design, it would be logical to compare the coaxial-rotor results. The coefficient of power (C_{P}) value is in the 0.0001–0.0008 range, while the coefficient of thrust (C_{T}) is in the 0–0.008. These ranges are the results for untwisted blades. Considering the twisted blades, C_{P} is in the 0.0002–0.001 range, while C_{T} is between 0 and 0.01. In another study, Tang et al. [41] analysed the contra-rotating

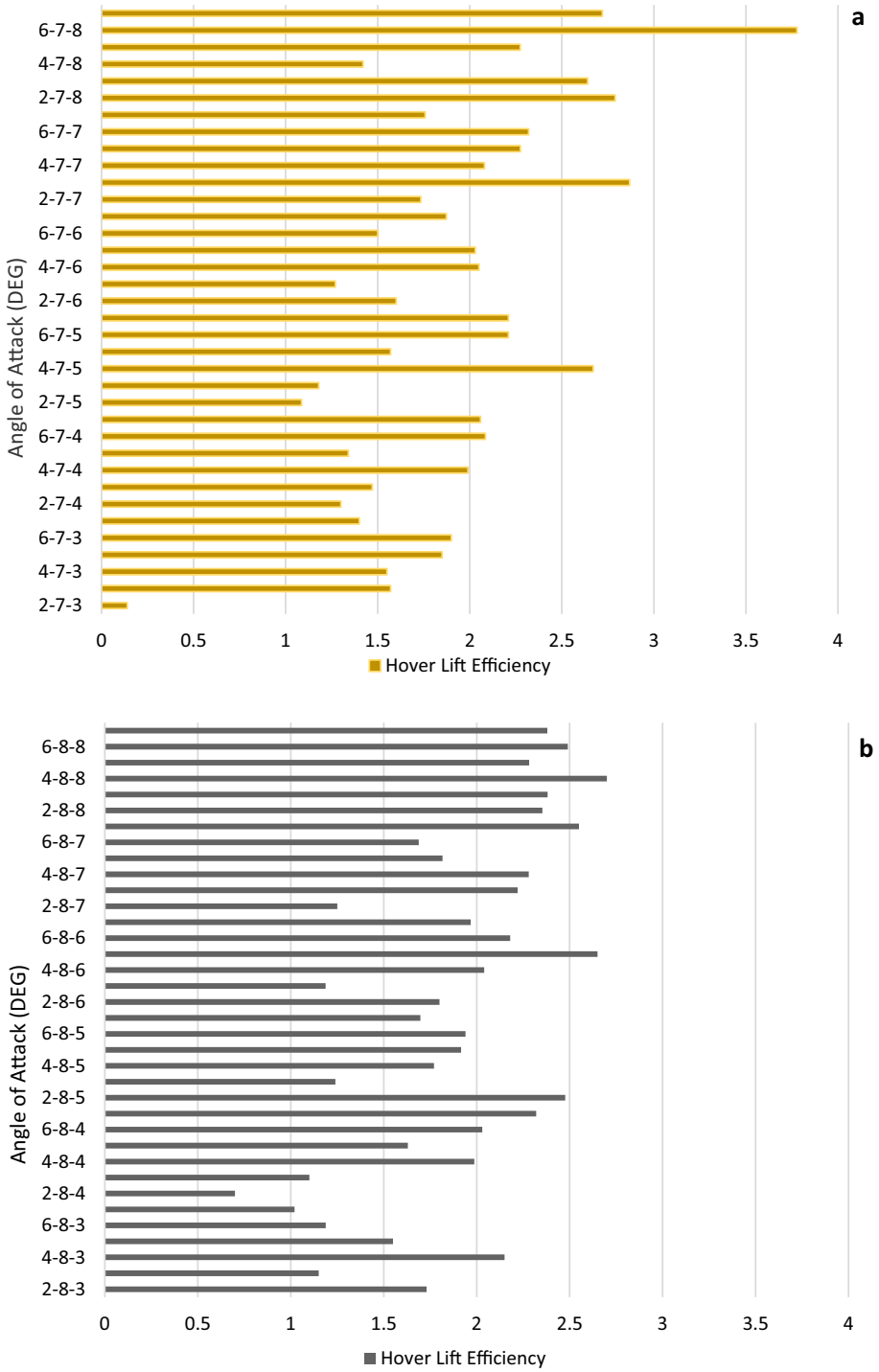

Fig. 17 The results obtained with the third propeller angle reduction (**a**) when the second propeller is 7 DEG and (**b**) when the second propeller is 8 DEG

propeller with high-lift airfoil S1223. CFD analysis gave them the efficiency of the design. C_T takes values between 0.03 and 0.13, and C_P values are between 0.006 and 0.0016. Gur [42] made a research on contra-rotating configuration. According to the Harrington test, C_T values are from 0 to 0.006 and C_P is between 0 and 0.0005. Haider et al. [43] studied single-rotor design for an agricultural unmanned helicopter. In this study, three types of blade configurations have been investigated. They used V1505A and V2008B airfoils on these configurations. Also, untwisted and twisted versions of these designs have been analysed. As a result, each design showed results in the same range of values: 0.3–1.2 for C_T and 0.04–0.26 for C_P. Finally, Kusyumov et al. [35] studied with a single rotor and made CFD analysis of the single-rotor propeller which was used NACA 0012 airfoil. It has been

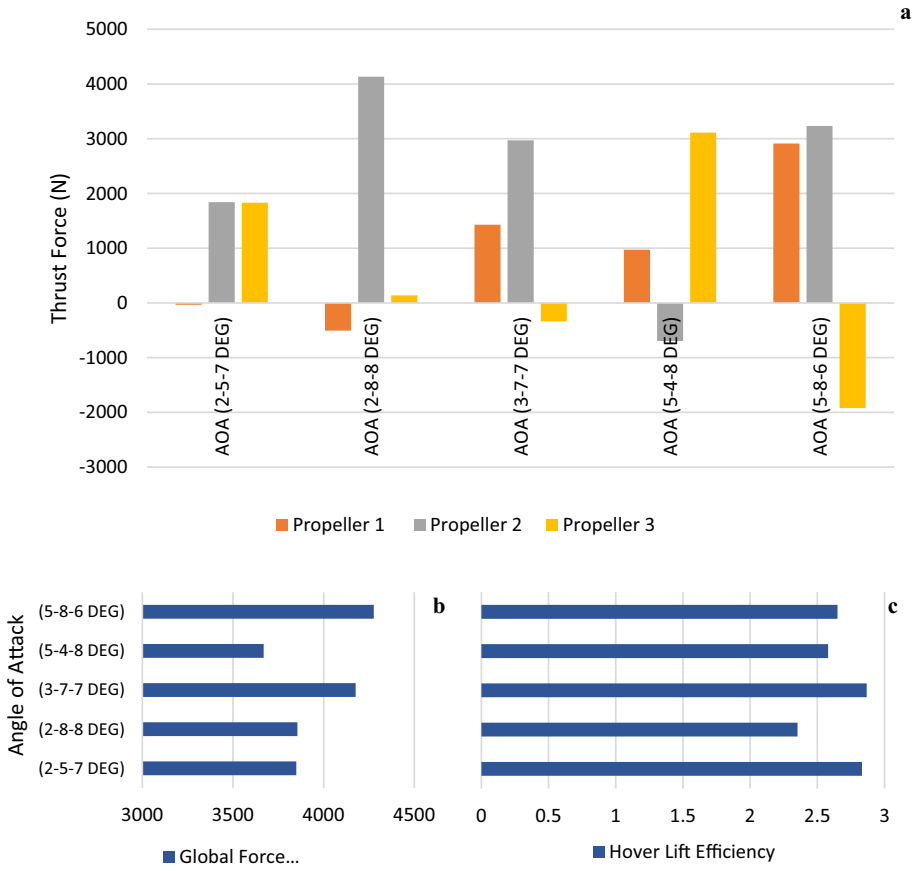

Fig. 18 **a** Thrust force graph, **b** global force graph, **c** hover lift efficiency graph when giving increment on AOA

found out when the thrust is equal to the weight of the helicopter, the thrust coefficient is equal to 0.0055. The graph in Fig. 22 shows that C_T has values around 0.005–0.018, while C_P is between 0.00055 and 0.00125. A comparison of our results with other studies is given in Table 10.

Moreover, C_T and C_P showed close results, especially with studies using the NACA0012 airfoil. An increment in torque is the result of raised induced power due to the induced drag at a high angle of attack [43]; these values are valid compared with other current studies with NACA0012 airfoil with both types of designs, twisted and untwisted. As a result, the results show similar results with a general range between 0.0001 and 0.0125 compared with the studies using NACA0012.

Finally, the numerical results of coefficients for sufficient angle-of-attack combinations shown an increment in values but not proportionally. The biggest reason for this pattern is the diversity in the angle-of-attack combinations, and this is more complicated in the triple rotor system. Coefficients of thrust and power represent similar results but as seen at some points an abnormal decrease in strength is observed at some combinations such as (3–6–7), (4–7–8), (6–6–7) and (7–7–7) (Fig. 23).

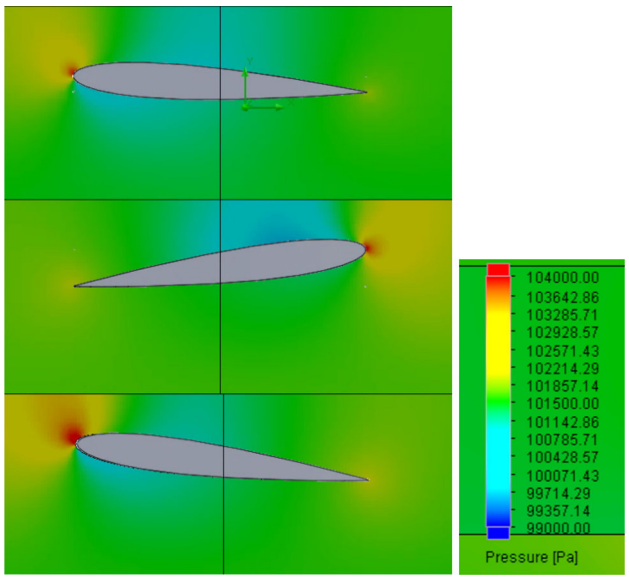

Fig. 19 Pressure distribution results of 3–7–7 DEG combination

4 Discussion

This study shows the results of the propeller design that used a symmetrical and untwisted basic airfoil. These results must

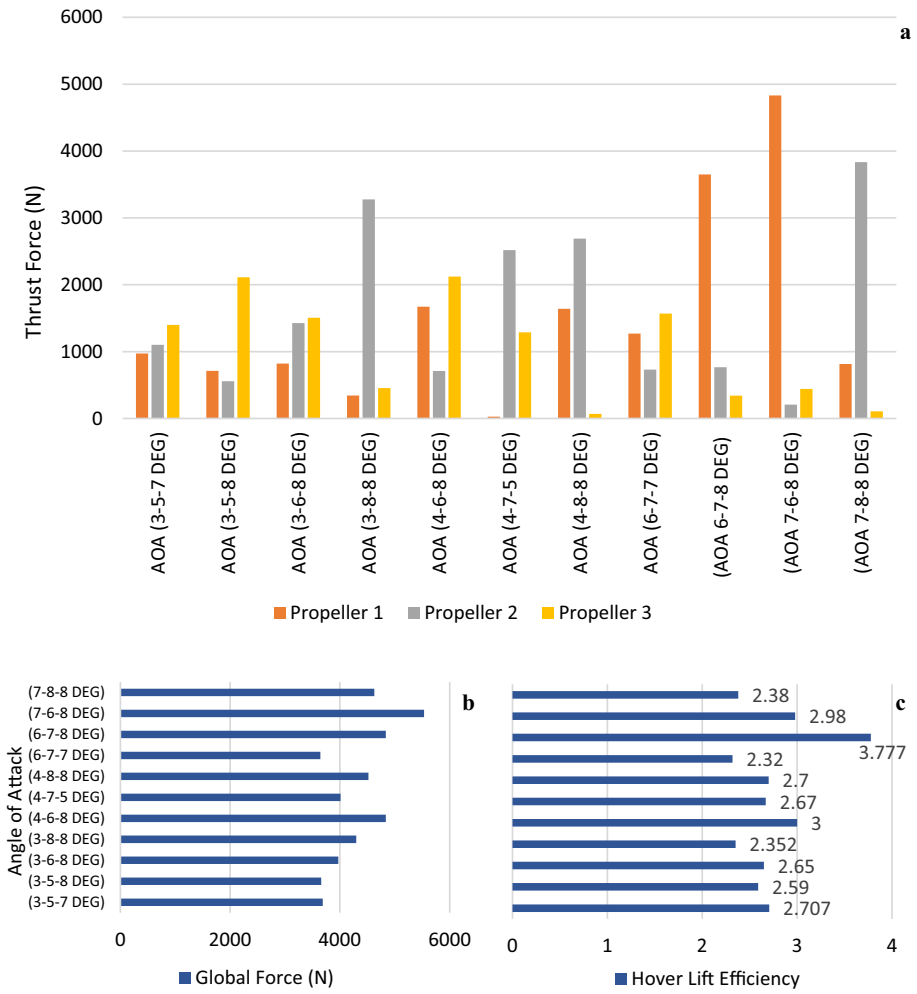

Fig. 20 **a** Thrust force graph, **b** global force graph, **c** hover lift efficiency graph

be considered according to the limitations of the NACA 0012 airfoil, especially regarding the angle of attack. As seen from the results, generally, one of the rotors gave negative thrust force in many tested combinations, even if the total force of the propeller is sufficient. Consequently, these outputs showed that the results are not constant for these specific variables and settings. But still, this design gave us some major information to understand the performance of a tri-rotor propeller in a wider aspect. Also, this basic design might be a pioneer of noticing out which points need to be improved in the multi-propeller design in the future.

5 Conclusions

The most important deduction that can be drawn from all the results shown is that the diameter of the rotor has decreased by 42.27% when compared with the single-propeller version of the same design parameters. The single-propeller diameter value is calculated as 4.5 m for this study. This value gives us one of the important advantages of this system, the reduction in the frontal drag area. The results proved that even if this tri-rotor propeller system produces sufficient thrust for hovering, in many situations, there is a conflict between the second and third propeller which is stronger at high angle combinations (6 DEG, 7 DEG and 8 DEG for NACA 0012).

Additionally, the coaxial design does not manage to support the power to the total system all the time. One reason for this might be because of the lower propeller performing a prop wash for the upper unit [40]. That is the problem that shows the point that needs to be improved in this design. That is because only the second propeller needs to involve in balancing and creating thrust force in the opposite direction to the other two propellers. The only disadvantage compared to the dual contra-rotating rotor system is that two propellers need to be balanced with one.

Nevertheless, the entire system gave positive results and sufficient thrust force at a few intervals. By considering combinations where this conflict does not exist, a certain working area can be determined or the interactions between different types of airfoils can be studied. Consequently, this design has great potential, because the propellers compensate for each

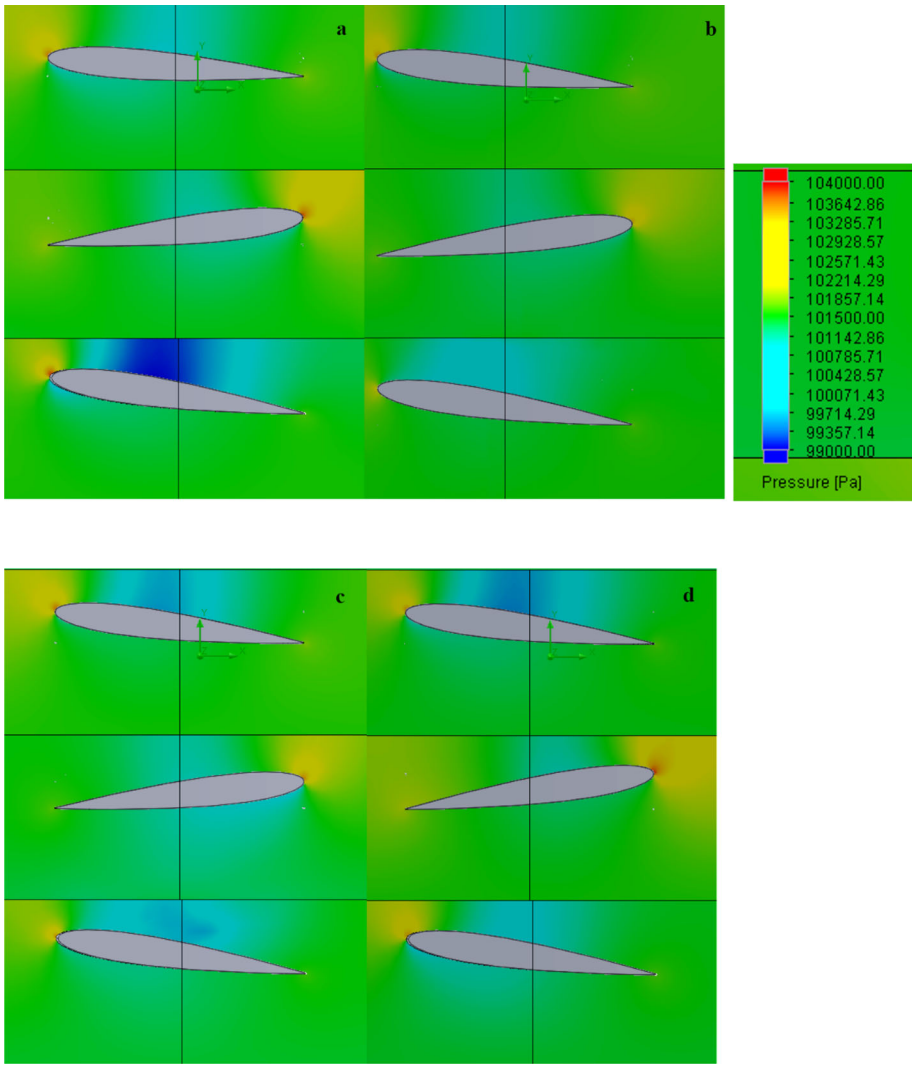

Fig. 21 The pressure distribution results of **a** 4–6–8 AOA combination, **b** 6–7–8 AOA combination, **c** 7–6–8 AOA combination and **d** 7–8–8 AOA combination

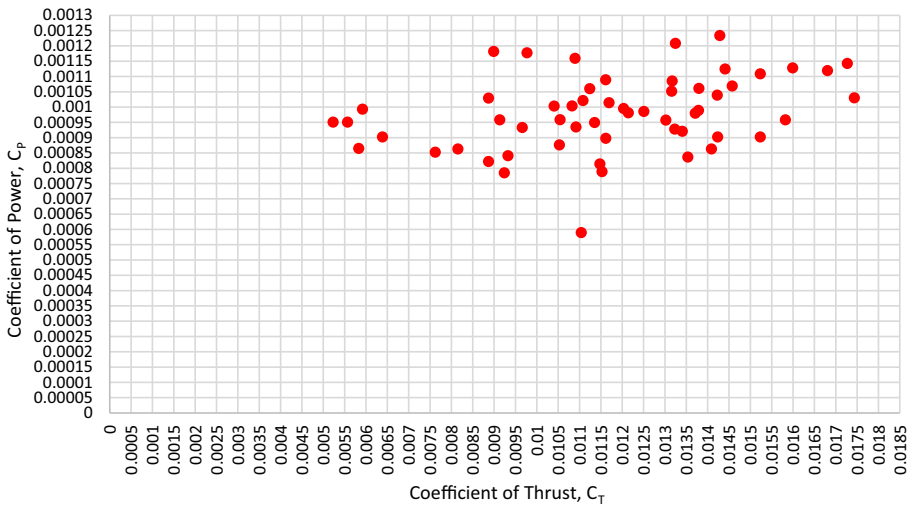

Fig. 22 C_T–C_P distributions of tri-propeller design with different angle-of-attack combinations

Table 10 Comparison of coefficients of the different kind of propeller design

	Configurations of rotor	Coefficient of torque (C_P)	Coefficient of thrust (C_T)	Airfoil type
Ramasamy [5]	Coaxial	0.0001–0.0008	0–0.008	Untwisted NACA0012
Ramasamy [5]	Coaxial	0.0002–0.001	0–0.01	Twisted NACA0012
Tang et. al. [41]	Coaxial	0.006–0.0016	0.03–0.13	high-lift airfoil S1223
Gur [42]	Contra-rotating	0–0.0005	0–0.006	NACA-4-digits symmetrical
Haider et.al. [43]	Single	0.04–0.26	0.3–1.2	Untwisted and Twisted Versions of V1505A and V2008B
Kusyumov et.al [35]	Single		0.0055	NACA0012
Current study	Tri-rotor coaxial contra-rotating	0.00055–0.00125	0.005–0.018	NACA0012

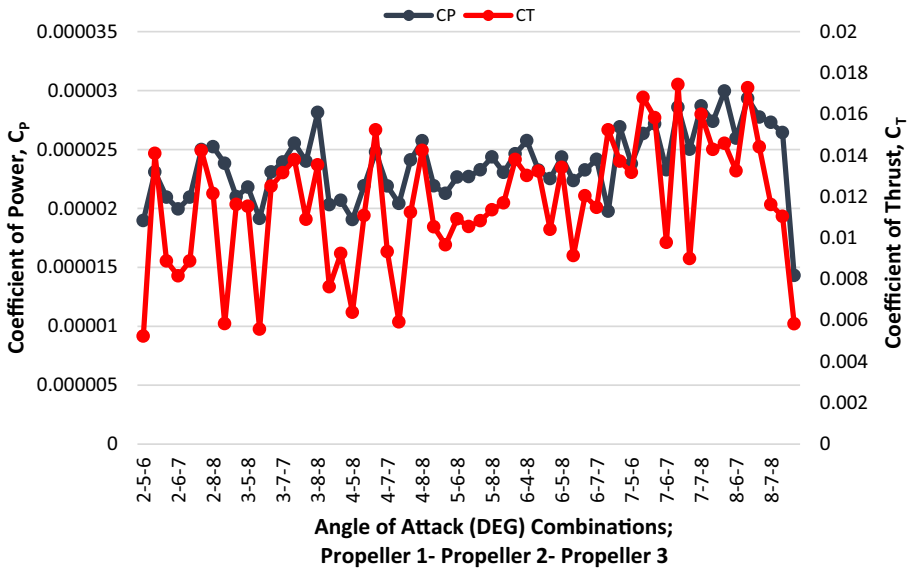

Fig. 23 Coefficient–angle-of-attack AOA graph

other's performance drops, just to eliminating instabilities. In addition, the results showed that at least two angles of increment between the propellers is the key point for better efficiency.

Author Contributions All authors contributed to the study conception and design. Material preparation, data collection and analysis were performed by LP and MS. The first draft of the manuscript was written by MS, and all authors commented on previous versions of the manuscript. All authors read and approved the final manuscript.

Funding Open access funding provided by Alma Mater Studiorum - Università di Bologna within the CRUI-CARE Agreement. The authors declare that no funds, grants, or other support was received during the preparation of this manuscript.

Data Availability The datasets generated during and/or analysed during the current study are not publicly available but are available from the corresponding author on reasonable request.

Declarations

Conflict of interest The authors have no relevant financial or non-financial interests to disclose.

References

1. Serrano, D.; Ren, M.; Qureshi, A.J.; Ghaemi, S.: Effect of disk angle-of-attack on aerodynamic performance of small propellers. Aerosp. Sci. Technol. **92**, 901–914 (2019). https://doi.org/10.1016/j.ast.2019.07.022
2. Bagai, A.: Aerodynamic design of the X2 Technology^{TM} demonstrator main rotor blade (2008)
3. Prior, S.D.: Reviewing and investigating the use of co-axial rotor systems in small UAVs. Int. J. Micro Air Veh. **2**(1), 1–16 (2010). https://doi.org/10.1260/1756-8293.2.1.1
4. Beaumier, P.: A low order method for co-axial propeller and rotor performance prediction. In: 29th Congress of the International Council of the Aeronautical Sciences, ICAS 2014 (2014)
5. Ramasamy, M.: Measurements comparing hover performance of single, coaxial, tandem, and tilt-rotor configurations. Annu. Forum Proc. AHS Int. **4**, 2439–2461 (2013)
6. Ferguson, K.; Thomson, D.: Performance comparison between a conventional helicopter and compound helicopter configurations. Proc. Inst. Mech. Eng. Part G J. Aerosp. Eng. **229**(13), 2441–2456 (2015). https://doi.org/10.1177/0954410015577997
7. Syal, M.; Leishman, J.G.: Aerodynamic optimization study of a coaxial rotor in hovering flight. J. Am. Helicopter Soc. **57**(4), 1–16 (2012). https://doi.org/10.4050/JAHS.57.042003
8. Qi, H.; Xu, G.; Lu, C.; Shi, Y.: A study of coaxial rotor aerodynamic interaction mechanism in hover with high-efficient trim model. Aerosp. Sci. Technol. **84**, 1116–1130 (2019). https://doi.org/10.1016/j.ast.2018.11.053
9. Moodie, A.; Yeo, H.: Design of a cruise-efficient compound helicopter. J. Am. Helicopter Soc. **57**, 1–11 (2012). https://doi.org/10.4050/JAHS.57.032004
10. Yeo, H.: Design and aeromechanics investigation of compound helicopters. Aerosp. Sci. Technol. **88**, 158–173 (2019). https://doi.org/10.1016/j.ast.2019.03.010
11. Jia, Z.; Lee, S.: Aerodynamically induced noise of a lift-offset coaxial rotor with pitch attitude in high-speed forward flight. J. Sound Vib. **491**, 115737 (2021). https://doi.org/10.1016/j.jsv.2020.115737
12. SKYbrary. Retreating Blade Stall. https://skybrary.aero/articles/retreating-blade-stall. Accessed 8 Nov 2022
13. Westbrook-Netherton, O.; Toomer, C.A.: An investigation into predicting vortex ring state in rotary aircraft. R. Aeronaut. Soc. (2015). https://doi.org/10.13140/RG.2.1.2294.5122
14. Stewart, W.: Helicopter behaviour in the vortex-ring conditions. Aeronaut. Res. Counc. Rep. Memo. No. 3117 (1959)
15. Pankhurst, R.C.; Veasy, B.A.; Greening, B.S.; Love, E.M.: Tests of contra-rotating propellers of 2-ft. diameter at negative pitch on a " typhoon " aircraft model, vol. 2218, p. 16 (1948)
16. Chaney, M.C.: The ABC helicopter. J. Am. Helicopter Soc. **14**(4), 10–19 (1969)
17. Paglino, V.M.: Forward flight performance of a coaxial rigid rotor (1971)
18. Preator, R.; Leishman, J.; Baldwin, G.: Performance and trade studies of a mono tiltrotor design (2005)
19. Playle, S.; Korkan, K.D.; von Lavante, E.: A numerical method for the design and analysis of counter-rotating propellers. J. Propul. Power **2**, 57–63 (1986)
20. Leishman, J.: Aerodynamic performance considerations in the design of a coaxial proprotor. J. Am. Helicopter Soc. **54**, 12001–12005 (2009). https://doi.org/10.4050/JAHS.54.012005
21. Coleman, C.P.: A Survey of Theoretical and Experimental Coaxial Rotor Aerodynamic Research (1997)
22. Ramasamy, M.: Hover performance measurements toward understanding aerodynamic interference in coaxial, tandem, and tilt rotors. J. Am. Helicopter Soc. **60**(3), 1–17 (2015)
23. Ferguson, K.: Towards a better understanding of the flight mechanics of compound helicopter configurations, p. 284 (2015)
24. Zhao, L.; Shkarayev, S.: Characterization of ducted contra-rotating propeller propulsions. Int. J. Micro Air Veh. (2019). https://doi.org/10.1177/1756829319837661
25. Maisel, M.D.; Giulianetti, D.J.; Dugan, D.C.: The history of the XV-15 tilt rotor research aircraft: from concept to flight. NASA Spec. Publ. **4517**, 194 (2000)
26. Walsh, J.L.; Bingham, G.J.; Riley, M.F.: Optimization methods applied to the aerodynamic (1987)
27. Piancastelli, L.; Sali, M.; Leon-Cardenas, C.: Basic considerations and conceptual design of a VSTOL vehicle for urban transportation. Drones **6**(5), 102 (2022)
28. Sogukpinar, H.: The effects of NACA 0012 airfoil modification on aerodynamic performance improvement and obtaining high lift coefficient and post-stall airfoil. AIP Conf. Proc. **1935**(February), 2–7 (2018). https://doi.org/10.1063/1.5025955
29. Srinivasa Rao, T.; Mahapatra, T.; Chaitanya Mangavelli, S.: Enhancement of lift-drag characteristics of NACA 0012. Mater. Today Proc. **5**(2), 5328–5337 (2018). https://doi.org/10.1016/j.matpr.2017.12.117
30. Javadi, A.; Pasandideh Fard, M.; Malek Jafarian, S.M.: Modification of k-ε turbulent model using kinetic energy-preserving method. Numer. Heat Transf. Part B Fundam. **68**, 554–577 (2015). https://doi.org/10.1080/10407790.2015.1065145
31. Harrington, R.D.: Full-scale-tunnel investigation of the static-thrust performance of a coaxial helicopter rotor. National Advisory Committee for Aeronautics, Vol. Technical, p. 24 (1951)
32. Xu, C.; Bil, C.; Cheung, S.C.P.: Fluid dynamics analysis of a counter rotating ducted propeller. In: 29th Congress of the International Council of the Aeronautical Sciences, ICAS 2014 (2014)
33. Chen, B.Y.; Reed, A.M.: A design method and an application for contrarotating propellers, No. August 1989 (1990)
34. NACA. ISA Atmosphere. Report 1235. https://www.digitaldutch.com/atmoscalc/. Accessed 9 Nov 2022
35. Kusyumov, A.N.; Mikhailov, S.A.; Batrakov, A.S.; Kusyumov, S.A.; Barakos, G.: CAA modeling of helicopter main rotor in hover. EPJ Web Conf. **143**, 1–6 (2017). https://doi.org/10.1051/epjconf/201714302060
36. Cameron, N.; Carter, D.: Rotorblade trailing edge flap failure modes and effects analysis. In: 35th European Rotorcraft Forum 2009, ERF 2009, vol. 1, pp. 134–148 (2009)
37. Uss, M.; Vozel, B.; Lukin, V.; Chehdi, K.: Exhaustive search of correspondences between multimodal remote sensing images using convolutional neural network. Sensors **22**, 1231 (2022). https://doi.org/10.3390/s22031231
38. Nersisyan, S.; Victor, N.; Galatenko, A.; Sokolov, A.; Bokov, G.; Konovalov, A.; Alekseev, D.; Tonevitsky, A.: ExhauFS: exhaustive search-based feature selection for classification and survival regression. PeerJ **10**, e13200 (2022). https://doi.org/10.7717/peerj.13200
39. Prasad Rao, J.; Holzsager, J.E.; Maia, M.M.; Diez, J.F.: Experimental study into optimal configuration and operation of two-four rotor coaxial systems for EVTOL vehicles. Aerospace **9**(8), 1–15 (2022). https://doi.org/10.3390/aerospace9080452
40. Bondyra, A.; Gardecki, S.; Gąsior, P.; Giernacki, W.: Performance of coaxial propulsion in design of multi-rotor UAVs. Adv. Intell. Syst. Comput. **440**, 523–531 (2016). https://doi.org/10.1007/978-3-319-29357-8_46

41. Tang, J.; Wang, X.; Duan, D.; Xie, W.: Optimisation and analysis of efficiency for contra-rotating propellers for high-altitude airships. Aeronaut. J. **123**(1263), 706–726 (2019). https://doi.org/10.1017/aer.2019.14
42. Gur, O.: Extending blade-element model to contra-rotating configuration. IOP Conf. Ser. Mater. Sci. Eng. **638**, 1 (2019). https://doi.org/10.1088/1757-899X/638/1/012001
43. Haider, B.A.; Sohn, C.H.; Won, Y.S.; Koo, Y.M.: Aerodynamically efficient rotor design for hovering agricultural unmanned helicopter. J. Appl. Fluid Mech. **10**(5), 1461–1474 (2017). https://doi.org/10.18869/acadpub.jafm.73.242.27541